Thermal expansion of the Ag(110) surface studied by low-energy electron diffraction and density-functional theory

V. B. Nascimento,* E. A. Soares, V. E. de Carvalho, E. L. Lopes, and R. Paniago

Departamento de Física, ICEx, UFMG, Caixa Postal 702, 30123-970 Belo Horizonte, MG, Brazil

C. M. C. de Castilho

Instituto de Física, UFBA, Campus da Federação, 40210-340 Salvador, BA, Brazil

In this work we present the results concerning the investigation of the temperature dependence of the first three interlayer spacings of Ag(110) surface using low energy electron diffraction (LEED) analysis and density-functional theory and molecular dynamics over a wide temperature range. It was possible to observe significant changes in the thermal expansion of the first and second interlayer distances without detection of effects associated with an enhanced anharmonicity. The values of the Debye temperature of the first two layers were obtained by LEED and a comparison between these results and those from other techniques are presented and discussed.

I. INTRODUCTION

Recently, the thermal behavior of fcc metal surfaces has gained more attention as a result of several interesting properties that have been revealed by both experimental and theoretical studies. Experimental techniques based on ion scattering, electron diffraction, energy-loss spectroscopy, and atom scattering, as well as theoretical methods such as density-functional theory (DFT) and embedded-atom method molecular dynamics (MD), have been used to investigate the enhancement of surface vibration anharmonicity, large anomaly in the surface thermal-expansion coefficient, the occurrence of roughening and premelting as the temperature is increased, and the behavior of the surface relaxation as the temperature is varied.[1–16] The analysis of the surface vibration modes can reveal the driving mechanism for thermal expansion, phase transitions, crystal stability, and surface diffusion anisotropy.[17] In the very recent few years, investigation has been done on the mechanism governing adatom diffusion on metal surfaces, in order to understand how to control the formation of low-dimension nanostructures on crystal surfaces. On the other hand, the noble metals have been used extensively as commercial catalysts and electrodes, where metallic surfaces play a key role. It is, therefore, crucial to understand the properties of these surfaces and their behavior under temperature variation.

The fact that bulk translational symmetry is broken when a crystal surface is created (e.g. by cleavage) implies that an anharmonic behavior of the restoring forces should be expected. So, if that happens, it must be possible to observe the occurrence of large atomic vibrational amplitudes,[3,6,8,12] anomalous thermal expansion,[1,2,4,6,8] finite phonon lifetimes,[11–13] surface melting, and roughening transitions,[3,9,10] and compare to properties of the bulk. It has been shown that these phenomena are dependent on the surface orientation and, for the fcc crystals, the (110) surface is expected to show the most intense effects.[7] For many elements the (110) surface of the fcc crystal shows a significant oscillatory multilayer relaxation for the first three or four

surface layers, a fact which is not observed for the other low-index faces (100) and (111). This results in a quite large contraction of the first interlayer spacing and a small expansion of the second one. It has been reported that these contraction and expansion can be exchanged as the temperature is varied.[17] The Ag(110) surface, the most open surface among the three low-index Ag surfaces, shows this kind of relaxation and therefore some anharmonicity enhancement could be expected for this surface.

The thermal behavior of the Ag(110) surface has been intensively studied over the last decade. Theoretically, different approaches have been used to study lattice dynamics,[18–20] structural and electronic properties,[21–23] thermal expansion,[24] the effect of the surface defects on the atomic vibration amplitudes,[25,26] and the diffusion of Ag atoms on the Ag(110) surface.[27] Experimentally, since the earlier observation of the oscillatory relaxation by high-energy ion scattering[28] (HEIS) and low-energy electron diffraction (LEED),[29,30] the Ag(110) surface has been examined by techniques such as impact-collision ion scattering and low-energy (medium-energy) ion scattering [L(M)EIS],[31–34] electron energy-loss spectroscopy,[35,36] He-atom scattering,[17,37] scanning tunneling microscopy,[38–40] and x-ray scattering.[41,42]

The idea that surface atoms undergo an increase in anharmonicity as the temperature is increased has been subject of intensive investigations. Specially for Ag(110) surface, several works have been performed in order to correlate anharmonicity, roughening transition, and premelting. In this way, the main issue has been the formation of point defects (vacancies and adatoms) in the first and second layers. Ion[33,34] and He-atom scattering[17] experiments have lead to the conclusions that Ag(110) disorder starts at about 600 K, due to the proliferation of thermally induced defects and a strong increasing of the diffusion coefficient is expected in the $\langle 1\bar{1}0 \rangle$ direction. Theoretically, several works, based mainly on molecular-dynamics simulations,[24,26,27] present results that reinforce the experimental conclusions about the ther-

mally induced defects, specially vacancies and adatoms. According to Devyatko and Rogozhkin[26] calculations for Ag(110) at 600 K, the vacancy-adatom pair concentration reaches 10%. They have concluded that the vacancy formation plays a key role and changes the surface properties such as an enhancement on the atomic vibrations. In a more recent work, Franchini *et al.*[24] carried out calculations based on a perturbative-theory approach, including third-order terms in the phonon-phonon interaction and a semiempirical force constant potential that allows inclusion of anharmonic effects to evaluate quantitatively the temperature dependence of the interplanar spacing. They have explored two models and, for one of them, they found the d_{12} and d_{23} thermal behavior in agreement with those from MEIS. However, they have pointed out that this temperature dependence is strongly related to how the anharmonicity between layers is treated. In addition, Narasimhan,[19] using *ab initio* calculations to obtain the bulk and surface interatomic force constant (frozen-phonon method), found that the radial force constant coupling the nearest-neighbor atoms in the first layer is softened by 12%, and in the case of the bonds coupling the first two layers, the force constant is stiffened by 15% with respect to those of bulk. However, a more pronounced change was observed in the radial force constant, which couples atoms from the first layer to those lying in the third layer. This parameter is enhanced by 37%. Based on those results, Narasimhan has also suggested that this large stiffening is responsible for the significant damping in the mean-square displacements in the *z* direction (taken as the one perpendicular to the surface plane), resulting into a larger in-plane displacement than at the normal direction to the surface. The author has also suggested that the large stiffening of the first to the third layer must have some impact on the thermal expansion of interlayer spacing and tends to keep d_{13} constant.

In spite of all these theoretical and experimental studies, the thermal behavior of the Ag(110) surface is still far from completely understood. For example, although several works predict an enhancement of anharmonic lattice vibrations as the temperature is increased, the exact harmonic-anharmonic transition temperature is not yet known. Also, the contraction-expansion transition of the first two layers, reported in some experimental and theoretical works,[18,31] and how it depends on the anharmonicity, requires more information. Then, additional investigations on the Ag(110) thermal-expansion behavior are still necessary.

In this work we present the results of the investigation of the temperature dependence for the first three interlayer spacings of Ag(110) surface using LEED analysis over a temperature range of 130–670 K and DFT *ab initio* molecular-dynamics calculations for the temperatures of 0 K, 60 K, 300 K, and 560 K. A comparison between these results and those from other techniques, as well as with those obtained for other fcc crystal faces, will be presented and discussed. The values of the Debye temperature of the first two layers were then obtained by LEED, within the process of searching the best fit between theoretical and experimental LEED-$I(V)$ curves. In Sec. II the experimental setup for data collection is presented while the theoretical details are shown in Sec. III. In Sec. IV the results are presented and discussed in Sec. V. The conclusions are presented in Sec. VI.

II. EXPERIMENT

The experiment was carried out in an ultra-high-vacuum chamber with LEED, Auger, cleaning and heating/cooling facilities at the Surface Physics Laboratory (DF-UFMG-Brazil). The silver crystal was supplied by the Monocrystal Company, with 99.995% purity and showing a mirrorlike (110) surface oriented within $\pm 1°$. The surface was cleaned by several cycles of sputtering/annealing (Ar^+ ions at 1.0 KeV, 450 °C, 30 min) until no carbon, oxygen, and sulphur could be detected by Auger spectroscopy. The sample temperature was monitored with a chromel-alumel thermocouple fixed at the sample holder but near the sample position. The LEED patterns were recorded at off-normal geometry ($\theta = 9.2°$ and $\phi = 67°$) using an Omicron LEEDStar video system for an energy range of 40–350 eV and sample temperatures of 133 K, 183 K, 229 K, 323 K, 523 K, 573 K, 623 K, and 673 K. At higher temperatures the LEED pattern could not be seen because the light coming from the heating filament increases the background enormously. The base pressure in the chamber was 5×10^{-10} mbars. The intensity versus energy curves [LEED-$I(V)$ curves] were collected for several diffracted beams, normalized with respect to the incident-beam current and smoothed using a five-point least-squares cubic polynomial algorithm. Despite the increase of the computational time required for the calculation of the theoretical LEED-$I(V)$ curves, an off-normal incidence geometry was chosen in order to increase the number of non-equivalent beams, specially at higher temperatures when the background intensity precludes a good data collection. The incidence angle was determined using the method developed by Cunninghan and Weinberg, as described by Van Hove *et al.*[43]

III. THEORETICAL DETAILS

The LEED analysis was carried out using a muffin-tin potential model for the silver crystal, with a muffin-tin radius of 1.45 Å being adopted for the Ag atoms. The muffin-tin potential and the phase shifts were calculated using the Barbieri/Van Hove phase-shift package.[44] In particular, a self-consistent Dirac-Fock approach was used to compute the self-consistent atomic orbitals for silver. The muffin-tin potential was then computed following Mattheiss' prescription and the relativistic phase shifts were evaluated by numerical integration of the Dirac equation. The theoretical LEED-$I(V)$ curves were calculated using the FSA-LEED program[45] running on a Pentium III 700-MHz, a K6 II 500-MHz, and an AMD-Athlon 1.3-GHz microcomputers running Linux. A set of eight phase shifts were used in the calculations and an inner potential of $V = (-10 + 4i)$ eV was assumed as a starting value. The cubic lattice constant *a* was corrected for temperature changes using the linear-expansion coefficient of $\alpha_{Ag} = 18.9 \times 10^{-6}$ K^{-1}, according to $a(T) = a(T_0)(1 + \alpha \Delta T)$, with $a(T_0) = 4.085$ Å (room temperature value).[46] The theory-experiment comparison was performed using the Pendry R factor.[47] For each temperature, the optimization of

TABLE I. Comparison between the structural and nonstructural parameters at 133 K, obtained in this work (second column) and the ones obtained by other experimental studies.

	LEED ($T=133$ K)	LEED (Ref. 29) ($T<100$ K)	HEIS (Ref. 28) (RT)	LEED (Ref. 30) (RT)
Δd_{12} (%)	(-7.9 ± 2.8)	(-7 ± 2)	-7.8	-5.7
Δd_{23} (%)	$(+3.6\pm4.2)$	$(+1\pm2)$	$+4.3$	$+2.2$
Δd_{34} (%)	(-0.9 ± 4.2)	(-2 ± 2)		
Δd_{45} (%)	Bulk	(0 ± 2)		
Θ_D (bulk) (K)	225	215	215	
Θ_{D1} (K)	150	150 (fixed)	149	
Θ_{D2} (K)	160	Bulk	149	
Final R_p	(0.16 ± 0.04)	0.18		

the structural and nonstructural parameters was performed in three steps. Initially, the first three surface interlayer distances (d_{12}, d_{23}, d_{34}), and the real part of the inner potential were allowed to relax while the Debye temperature of the surface layers were kept fixed at the bulk value ($\Theta_D = 225$ K). In the search for the best set of interlayer distances, the FSA approach[45] was the adopted procedure. Then, for the best set of interlayer distances, the Debye temperature of the first and second layers (Θ_{D1} and Θ_{D2}) were optimized by running calculations on a grid of values. Finally, a new optimization of the structural parameters (FSA approach) using the optimal surface Debye temperatures was carried out.

The *ab initio* calculations were performed within the density-functional theory using the local-density approximation (LDA) for the exchange-correlation potential.[48,49] The plane-wave pseudo-potential method was used, where the Ag atoms are described by ultrasoft pseudopotentials (USPP) generated with a scalar-relativistic calculation.[50] The DFT-LDA and molecular-dynamics calculations were carried out using the PWSCF computer package[50] running on a PC's Linux Cluster.[51]

IV. RESULTS

A. LEED analysis

In order to certify the quality of our experimental LEED data and the reliability of the LEED-$I(V)$ calculations, the first step was to verify the occurrence of the expected oscillatory relaxation for the lowest-temperature dataset ($T = 133$ K). As shown in Table I, our results are in reasonable agreement with those reported in the literature.[28–30] In Fig. 1 we present a theory-experiment comparison for some LEED-$I(V)$ curves, in the case of $T = 133$ K. It can be seen from this figure, and confirmed by the low-R_P values, that a very good agreement between theory and experiment was achieved. After that, the analysis was repeated for all the sample measured temperatures and the results are summarized in Table II. The behavior of the first three interlayer spacings, as the temperature is varied, is represented in Fig. 2. As can be seen from this figure, the first interlayer spacing d_{12} undergoes a contraction, which decreases as the temperature goes up. The second interlayer spacing d_{23} expands but also goes down as the temperature increases, while the third
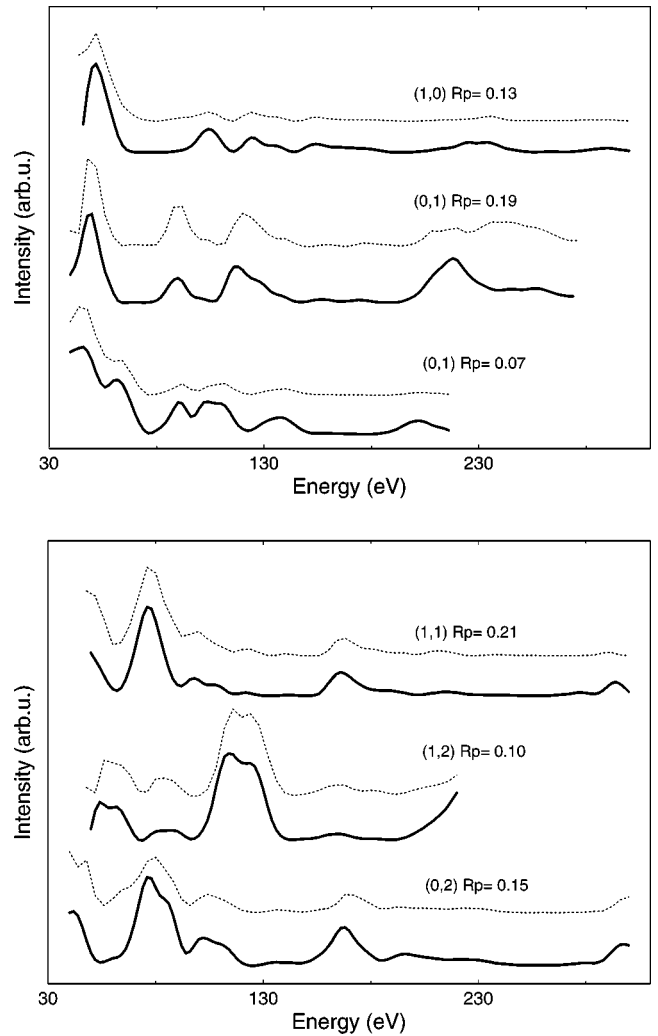
FIG. 1. Comparison between some theoretical and experimental LEED-$I(V)$ curves for the Ag(110) dataset collected at $T = 133$ K. The more defined lines corresponds to the experimental LEED-$I(V)$ curves. For each pair of curves the beam index and the final R_P factor are presented.

TABLE II. The percentage of the interlayer spacing variation with the sample temperature as a result of the LEED analysis. The effective Debye temperature is also shown for each surface temperature. R_P is the final Pendry R factor in the structural determination. ''Beams'' corresponds to the number of beams used in each temperature and the ΔE_T is total range of energy defined by the experimental beams. $T_M = 1234$ K is the Ag melting point.

T(K)	T/T_M	Δd_{12} (%)	Δd_{23} (%)	Δd_{34} (%)	Θ_{D1} (K)	Θ_{D2} (K)	R_P	Beams	ΔE_T (eV)
133	0.11	(-7.9 ± 2.8)	$(+3.6\pm4.2)$	(-0.9 ± 4.2)	(150 ± 65)	160	0.16	9	1900
183	0.15	(-6.9 ± 3.0)	$(+1.4\pm4.2)$	(-0.2 ± 4.2)	150	150	0.19	9	1900
229	0.18	(-8.5 ± 3.5)	$(+2.5\pm4.2)$	(-2.1 ± 5.0)	155	175	0.22	9	1980
323	0.26	(-7.8 ± 3.5)	$(+3.5\pm4.8)$	(-1.5 ± 4.5)	(155 ± 90)	175	0.21	9	1854
523	0.42	(-7.0 ± 4.1)	$(+2.1\pm6.0)$	(-3.3 ± 8.0)	200	200	0.20	9	994
573	0.46	(-5.8 ± 2.8)	$(+3.0\pm4.8)$	(-1.9 ± 9.6)	190	210	0.19	9	552
623	0.50	(-1.3 ± 3.5)	(-5.3 ± 4.2)	$(+2.4\pm9.5)$	160	180	0.21	9	354
673	0.55	(-0.2 ± 6.5)	(-0.7 ± 8.0)	$(+2.5\pm10.0)$	(170 ± 100)	200	0.20	8	284

interlayer spacing d_{34} shows a contraction at low temperatures (133–573 K), which is converted into a small expansion at higher temperatures.

The Debye temperatures, as determined from the LEED calculations for each temperature, are shown in Table II. These were essentially constant over the measured temperature range, within the precision of the measurements. The average Debye temperatures from this analysis were 166 $\pm$ 15 K and 181 $\pm$ 17 K for the first two layers, respectively. The uncertainties in the surface Debye temperature are the standard deviations with respect to the mean value.

B. DFT calculations

In order to check the validity of the silver USPP used in this work, calculations of some of the Ag bulk properties were performed. First, to determine the bulk equilibrium lattice constant a_0 and the bulk modulus B_0, a series of static total-energy calculations, as a function of the lattice parameter, using different values for the plane-wave kinetic-energy cutoff E_{cut} and the Monkhorst-Pack grid used in the Brillouin-zone integration, were carried out. The equilibrium lattice constant and the bulk modulus were then obtained by fitting the results to a Murnaghan's equation of state[52] (Table III). In Fig. 3(a) the static total energy as a function of the lattice parameter, as well as Murnaghan's fit, is shown for

two different calculations. As can be seen from this figure and from Table III, the values for a_0 and B_0 are basically independent of E_{cut} and the grid size. The resulting values of $a_0 = 4.01$ Å and $B_0 = 1.14$ Mbar deviate from the experimental values by 1.7% and 13%, respectively, and agree well with other theoretical results.[23,55] Using the lattice parameter corresponding to a static equilibrium, electronic density of states and the phonon-dispersion curves, using $E_{cut} = 25$ Ry and a grid of $(10\times10\times10)$, were calculated. The results of both calculations are shown in Figs. 3(b) and 3(c) and are also in good agreement with the experimental results. In particular, the phonon-dispersion curves are in excellent agreement with results from the calculations performed by Xie *et al.*[55] and Narasimhan.[19]

The Ag(110) surface calculations were performed using a repeating slab geometry, consisting of seven or nine layers of atoms separated by a vacuum of thickness equivalent to 16 atomic layers and a $(8\times8\times1)$ grid in the Brillouin zone. The equilibrium geometry was obtained by fully relaxing all the atomic layers in the slab using the Broyden-Fletcher-Goldfarb-Shanno algorithm.[56] Relaxing all the slab layers gives an extra convergence check since at equilibrium the interlayer distances on both sides of the slab have to be identical. The structural parameters, resulting from the geometry optimization at 0 K are presented in Table IV, as well as

FIG. 2. The percentual change in the first three interlayer spacings as a function of the surface temperature (normalized to the melting temperature $T_M = 1234$ K) obtained by LEED.

TABLE III. Equilibrium lattice parameter and the bulk modulus for several values of E_{cut} and grid size.

E_{cut} (Ry)	Grid	a_0 (Å)	B_0 (Mbar)
25	$(8\times8\times8)$	4.01140	1.14283
50	$(8\times8\times8)$	4.01120	1.14236
60	$(8\times8\times8)$	4.01120	1.14240
70	$(8\times8\times8)$	4.01110	1.14240
80	$(8\times8\times8)$	4.01110	1.14240
25	$(10\times10\times10)$	4.01100	1.14375
50	$(10\times10\times10)$	4.01100	1.14373
60	$(10\times10\times10)$	4.01100	1.14378
70	$(10\times10\times10)$	4.01100	1.14377
80	$(10\times10\times10)$	4.01100	1.14377
Experimental values (Ref. 46)		4.085	1.00
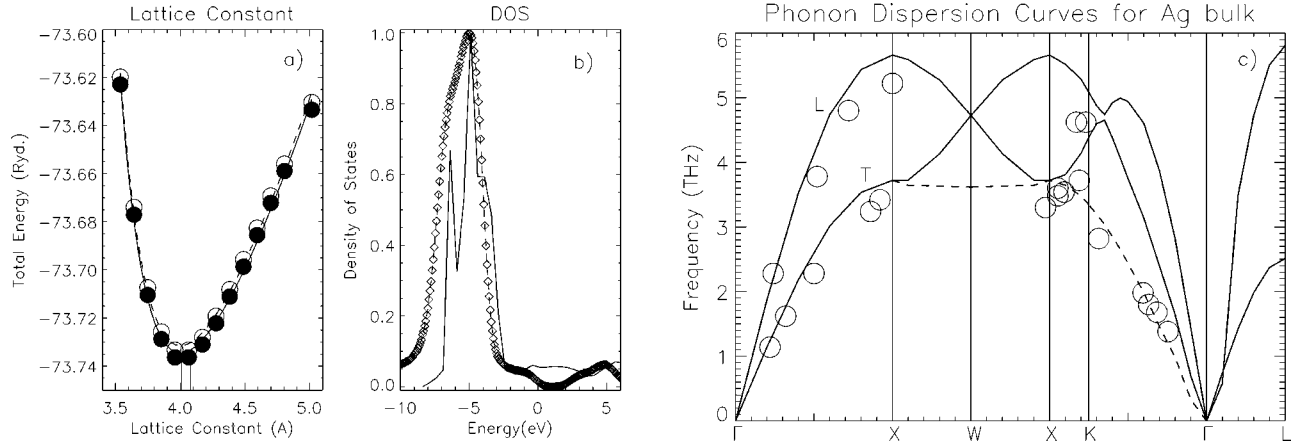
FIG. 3. (a) Static total energy per atom as a function of the lattice parameter a for the Ag bulk. Open circles correspond to the results for $E_{cut} = 25$ Ry and a $(8 \times 8 \times 8)$ grid and full circles to $E_{cut} = 80$ Ry and a $(10 \times 10 \times 10)$. (b) Experimental (Ref. 53) (diamonds) and calculated (solid line) electronic density of states for the Ag bulk [$E_{cut} = 25$ Ry and a $(10 \times 10 \times 10)$ grid]. (c) Calculated phonon-dispersion curves at the lattice parameter corresponding to static equilibrium. Experimental neutron data (Ref. 54) are represented by the open circles. T and L stand for transverse and longitudinal modes, respectively.

those from other theoretical studies.[19,23] As can be seen, there is a very good agreement between the experimental and theoretical results presented in Tables I and IV.

After determining the Ag(110) structure at 0 K, molecular dynamics simulations (DFT-MD) were performed on the Born-Oppenheimer surface at three different surface temperatures (60 K, 300 K, and 560 K) using the Verlet algorithm. After each time step, a self-consistent calculation was performed in order to obtain the new electronic charge density. In all simulations a time step of 3.87 fs was used and a total simulation time of 3 ps was achieved. The time step was carefully chosen in order to guarantee energy conservation. The changes in the first and second interlayer distances, obtained by the DFT-MD simulations, are presented in Fig. 4. It can be seen from this figure that the DFT-MD results obtained in this work are in reasonable agreement with the results obtained by LEED and with results from other theoretical and experimental studies.

V. DISCUSSION

In order to compare our results with those from the literature, in Fig. 4 the LEED and DFT-MD data together with those from a MEIS experiment[31] as well as those from classical molecular-dynamics simulation[18] (MD) for the first and second interlayer spacings (d_{12} and d_{23}) are plotted. It is clear from this figure that the LEED, MD, and DFT-MD data show two "regions:" a nearly constant expansion coefficient at low temperatures which suddenly presents an increasing behavior at high temperatures. This change occurs for the LEED data at about 0.45 T_M. In an attempt to quantify the differences between the datasets shown in this figure, the linear-expansion coefficient for the first interlayer distance was obtained through a linear fitting of the data in the temperature range for which $d_{12}(T)$ shows a nearly linear behavior (except for the DFT-MD results where all the points were used). The results then obtained for the linear expansion coefficients are $\alpha_{LEED} = (60 \pm 20) \times 10^{-6}$ K^{-1}, $\alpha_{DFT-MD} = (98 \pm 50) \times 10^{-6}$ K^{-1}, $\alpha_{MEIS} = (402 \pm 30) \times 10^{-6}$ K^{-1}, and $\alpha_{MD} = (80 \pm 5) \times 10^{-6}$ K^{-1}. The MEIS results show, for d_{12}, a contraction that changes to an expansion at about $T = 550$ K ($0.45 T_M$) and a very high expansion coefficient (about 21 times larger than the bulk). On the other hand, the MD results show a contraction up to $T \sim 700$ K and a comparatively lower expansion coefficient (four times larger than the bulk). The LEED and DFT-MD results are in better agreement with those from MD study, with an expansion coefficient of about three and five times the bulk value, respectively. Therefore, the LEED analysis does not show an

TABLE IV. Comparison between the equilibrium geometry of the Ag(110) obtained in this work and other theoretical results. USPP stands for ultrasoft pseudopotential and NCPP for norm conserving pseudopotential.

	This Work		Wang *et al.* (Ref. 23)		Narasimhan (Ref. 19)
Δd_{12} (%)	-8.04	-8.03	-8.81	-9.19	-6.9
Δd_{23} (%)	$+3.79$	$+4.17$	$+3.59$	$+4.10$	$+2.3$
Δd_{34} (%)	-0.55	-0.85	-1.11	-1.50	-1.2
Atomic layers	7	9	11	11	7
Vacuum layers	16	16	9	9	5
Potential	USPP	USPP	USPP	USPP	NCPP
	LDA	LDA	LDA	GGA	LDA
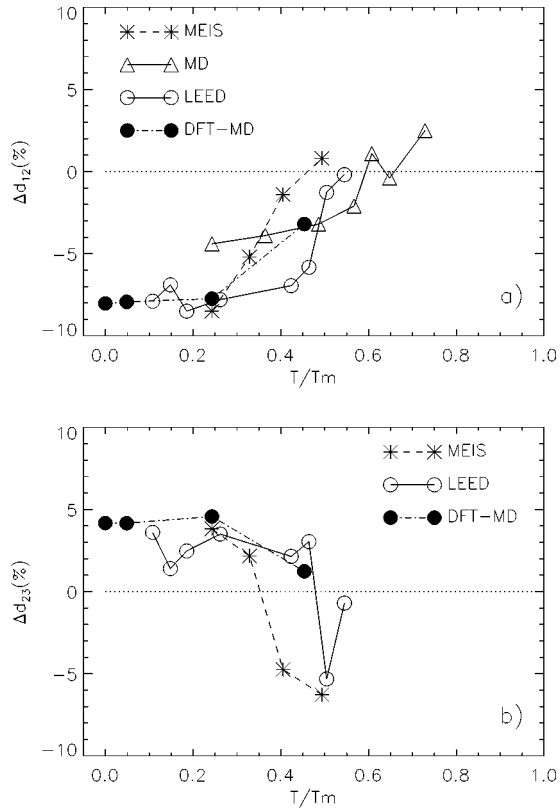
FIG. 4. (a) Thermal expansion of the first interlayer spacing obtained by LEED, DFT-MD, MEIS (Ref. 31), and molecular dynamics (MD) (Ref. 18). (b) The same for the second-layer expansion.

anomalous expansion coefficient for the first interlayer spacing of Ag(110) surface at least up to $0.45T_M$. Furthermore, the LEED data for the second interlayer spacing d_{23} do not agree with those from MEIS analysis, as can be seen in Fig. 4(b). Again, an expansion/contraction transition for this parameter, at about 430 K ($0.35T_M$), is shown in the MEIS results, whereas from the LEED data the parameter undergoes an expansion, although decreasing, up to about 600 K ($0.49T_M$). This lack of coincidence between MEIS and other techniques results was previously observed for the (111) silver surface, either by LEED (Ref. 14) or by x-rays.[15]

In the temperature range up to $0.45T_M$, the LEED results do not indicate the occurrence of an contraction/expansion transition. However, at higher temperatures ($T > 0.45T_M$), the LEED results show a more rapid increase of the d_{12} interlayer distance in such a way that at 673 K this distance is very close to the bulk value. The linear-expansion coefficient in this temperature range changes drastically from $\alpha_{LEED} = (60 \pm 20) \times 10^{-6}$ K^{-1} to $\alpha_{LEED} = (780 \pm 20) \times 10^{-6}$ K^{-1} and it is even greater than that of MEIS experiment. The d_{23} interlayer distance also shows a different behavior at this higher temperature range (Fig. 4).

It has been argued that a rapid increase in surface expansion should be due to a strong surface anharmonicity, which could lead to an instability at the surface and premelting.[1,57,12,13,18] According to the Debye model, a linear behavior of the mean-square displacements of the surface

atoms with respect to the temperature is expected. In fact, this has been observed in an ion scattering experiment on Ag(110) surface[33] for a temperature range below 600 K. Above 600 K a different behavior for the mean-square displacements was observed. Therefore, a different value of the surface Debye temperature for $T > 600$ K should be expected. In the present LEED analysis of the Ag(110), an optimization of the effective Debye temperature for the first two surface layers has been accomplished and the results (see Table II) show that, for both layers, the Debye temperature does not change as the sample temperature is varied, at least in the investigated temperature range (from 133 K up to 673 K). These two parameters show small variations around the mean values of $\Theta_{D1} = 166$ K and $\Theta_{D2} = 181$ K for the first and second layers, respectively. These values are lower than those reported by Devyatko and Rogozhkin,[26] of 205 K, for the first layer and higher than those reported by Bracco *et al.*[33] in an ion scattering experiment, where they found $\Theta_{\langle 1\bar{1}0 \rangle} = 140$ K and $\Theta_{\langle 001 \rangle} = 116$ K for the $\langle 110 \rangle$ and $\langle 001 \rangle$ azimuths, respectively. However, based on the bulk value of $\Theta_D = 225$ K that has been used in our LEED calculation, the value of Θ_{D1} is in good agreement with that one expected (159 K) from the theoretically simple expression $\Theta_{surf} = \Theta_{bulk}\sqrt{2}/2$. These results are consistent with the linear behavior of the mean-square displacement with temperature in the whole investigated temperature range, as predicted by the Debye model. Therefore, based on the present LEED analysis, the rapid increase above 556 K ($0.45T_M$), of the Ag(110) first interlayer distance seems not to stem from anharmonic effects. However, it must be mentioned that in the present LEED analysis anisotropy in the surface atom vibrations was not taken into account and so, the values found for the surface Debye temperature represent only effective values. In addition, as can bee seen from Table II, the two first layers show nearly the same value for the Debye temperature and lower than the bulk value, that is, $\Theta_{D1} = 166$ K and $\Theta_{D2} = 181$ K. In a similar LEED analysis for Ag(111) surface, Soares *et al.*[14] have obtained more distinct values ($\Theta_{D1} = 165$ K and $\Theta_{D2} = 199$ K), indicating a larger stiffness of the second layer with respect to the first one. However, for Ni(110) (Ref. 58) at $T = 198$ K $\Theta_{D1} = 240$ K and $\Theta_{D2} = 260$ K were obtained, where a value of $\Theta_D = 350$ K for the bulk value was used in the calculation, and for Ni(111) (Ref. 59) $\Theta_{D1} = 240$ K and $\Theta_{D2} = \Theta_{DBulk}$ were obtained. Based on these results, it seems that in the (111) surface the first and second layers show a more distinct set of values for the Debye temperature than the (110) one. These may happen because the (110) is the more open low-index surface and the two first layers are nearly equally free to oscillate.

The study of the Ag(110) thermal behavior has been carried out mainly considering the formation of point defects such as vacancies and vacancy-adatom pairs using different experimental techniques and theoretical approaches. The main results from these works have emphasized the correlation between defect formation and thermal anharmonicity. The present LEED analysis does not give information about the formation of surface defects and therefore it is difficult to draw any conclusion about this process except that anharmonicity (if that occurs) should appear on the dependence of the

Debye temperature with temperature as obtained by LEED. The results of the present work show only nearly constant values for Θ_{D_1} and Θ_{D_2}, then it might be an indication that anharmonic effects are at most small in the explored temperature range.

On the other hand, Narasimhan's work[19] suggests that the Ag(110) thermal expansion may be controlled by a large stiffening of the first to the third layer, which tends to keep d_{13} constant. We have examined this point, and as can be seen in Fig. 2 and Table II, the d_{13} distance undergoes a contraction of -0.06 Å (-2.2%) at 133 K, becoming -0.01 Å (-0.4%) at 673 K. However, the standard deviation $\langle \Delta d_{13} \rangle$ calculated with respect to the mean value $\langle d_{13} \rangle$ $=2.83$ Å is 0.03 Å (1.1%). So, the d_{13} distance behaves as nearly constant, within the error range, for the whole temperature range which was examined. Therefore, it may be concluded that the Narasimhan prediction may be a more general behavior for the Ag(110) surface, and this seems to be valid up to higher temperatures such as 673 K. Based on Narasimhan's work,[19] a possible explanation for the changes in the first and second interlayer distances may be suggested. In that study, *ab initio* calculations were performed in order to obtain the bulk and surface interatomic force constants (frozen-phonon method), and the results then obtained indicate that the radial force-constant coupling atoms from the first to the third atomic layers, relative to the bulk value, is enhanced by 37%. Besides that, the thermal vibrations of the second-layer atoms, along the z direction (normal to surface), are increased, relative to the bulk value, by a factor of 2.3. In addition to that, the in-plane thermal vibrations in the first layer also present a considerable enhancement in the amplitudes with respect to bulk along the $\langle 001 \rangle$ direction by a factor of 2.1. Based on these results, we suggest that with the increase of temperature, the enhanced second-layer thermal vibration amplitude along the z direction and the first layer in-plane vibrations will also increase, forcing d_{12} to expand. Due to the strong coupling between the first and third layers, the third layer will also move in an attempt to keep d_{13} constant. However, it seems that the origin of the driving force involved in a rapid increasing of the thermal expansion coefficient for $T>0.45T_M$ is still not understood. The dynamics of the first layer atoms is controlled by the surface force constants, which depend on the charge distribution on the surface. In this way, surface states may play an important role in the surface force equilibrium. The Ag(110) surface has a Shockley-type surface state in a gap at the Y zone boundary of the surface Brillouin zone. At room temperature it lies at 0.06 eV below the Fermi energy E_F. It has been shown by ultraviolet photoemission spectroscopy[60] and, more recently, by second-harmonic generation, measurements[61] that this state has a linear dependence on the energy with the surface temperature. Based on this linear behavior, it can be inferred that the surface-state energy crosses the Fermi level at about 624 K and becomes completely unoccupied above this temperature ($T>0.50T_M$). Then, we speculate that the loss of a surface state charge may induce to a new force equilibrium conditions within the surface layer(s) that drives the abrupt change in the interlayer spacing. This point requires more investigation and perhaps it will put some more light on the intriguing behavior of the thermal expansion of the Ag(110).

Therefore, from the LEED analysis, it can be concluded that in the entire investigated temperature range, i.e., from 133 K to 673 K, there is no evidence of any effect related to an enhancement in anharmonicity which could give rise to the observed anomalous thermal expansion, occurring at about $T=0.45T_M$.

The DFT-MD simulations also show a reduction of the first layer distance from -8.03% at 0 K to -3.4% at 560 K, indicating that a contraction/expansion transition might occur for temperatures higher than 600 K. However, it is not possible to say when the contraction starts decreasing since no simulations were carried out between 300 K and 560 K as a result of computing time limitation. It is worth to be mentioned that the DFT-MD simulations and the LEED results obtained in this work are in good agreement, specially at lower temperatures.

VI. CONCLUSIONS

In this work we have used low-energy electron diffraction and density-functional calculations in order to study the thermal expansion of the Ag(110) surface from 60 K up to 670 K. Our results seem to support the MEIS main conclusion of an anomalous thermal expansion above $0.45T_M$. The results also show that the effective surface Debye temperature, as it was determined by this LEED analysis, is nearly constant for both first and second layers. Therefore, no anharmonicity could be inferred at least up to 600 K. As for other (110) fcc surfaces, the two first layers show nearly the same value for the Debye temperature.

---

*Corresponding author. Present address: Instituto de Física, UFBA, Campus da Federação, 40210-340, Salvador, BA, Brazil. Email address: von@ufba.br

[1] J.W.M. Frenken, F. Huussen, and J.F. van der Veen, Phys. Rev. Lett. **58**, 401 (1987).

[2] Y. Cao and E. Conrad, Phys. Rev. Lett. **65**, 2808 (1990).

[3] G. Helgesen, D. Gibbs, A.P. Baddorf, D.M. Zehner, and S.G.J. Mochrie, Phys. Rev. B **48**, 15 320 (1993).

[4] P. Statiris, H.C. Lu, and T. Gustafsson, Phys. Rev. Lett. **72**, 3574 (1994).

[5] L.J. Lewis, Phys. Rev. B **50**, 17 693 (1994).

[6] E.P. Gusev, H.C. Lu, E. Garfunkel, and T. Gustafsson, Surf. Rev. Lett. **3**, 1349 (1996).

[7] A. Kara, P. Staikov, A.N. Al-Rawi, and T.S. Rahman, Phys. Rev. B **55**, R13 440 (1997).

[8] K.H. Chae, H.C. Lu, P. Statiris, and T. Gustafsson, Surf. Rev.

Lett. **4**, 1091 (1997).

[9] M. Schwarz, C. Mayer, P. von Blanckenhagen, and W. Schommers, Surf. Rev. Lett. **6**, 1095 (1997).

[10] C.S. Jayanthi, E. Tosatti, and L. Pietronero, Phys. Rev. B **31**, 3456 (1985).

[11] J. Xie and M. Scheffler, Phys. Rev. B **57**, 4768 (1998).

[12] K. Pohl, J.-H. Cho, K. Terakura, M. Scheffler, and E.W. Plummer, Phys. Rev. Lett. **80**, 2853 (1998).

[13] A.N. Al-Rawi, A. Kara, and T.S. Rahman, Surf. Sci. **446**, 17 (2000).

[14] E.A. Soares, G.S. Leatherman, R.D. Diehl, and M.A. Van Hove, Surf. Sci. **468**, 129 (2000).

[15] C.E. Botez, W.C. Elliott, P.F. Miceli, and P.W. Stephens, Phys. Rev. B **63**, 113404 (2001).

[16] J. Xie, S. de Gironcoli, S. Baroni, and M. Sheffler, Phys. Rev. B **59**, 970 (1999).

[17] L. Pedemonte, R. Tatarek, M. Vladiscovic, and G. Bracco, Surf. Sci. **507**, 129 (2002); **510**, 134 (2002).

[18] T.S. Rahman and Z.J. Tian, J. Electron Spectrosc. Relat. Phenom. **64/65**, 651 (1993).

[19] S. Narasimhan, Surf. Sci. **496**, 331 (2002).

[20] T.S. Rahman, J.D. Spangler, and A. Al-Rawi, Surf. Sci. **502/503**, 429 (2002).

[21] K-P. Bohnen and K.M. Ho, Electrochim. Acta **40**, 129 (1995).

[22] I. Vilfan, F. Lanon, and E. Adam, Surf. Sci. **440**, 279 (1999).

[23] Y. Wang, W. Wang, K-N. Fan, and J. Deng, Surf. Sci. **490**, 125 (2001).

[24] A. Franchini, C. Magherini, and G. Santoro, Surf. Sci. **502/503**, 443 (2002).

[25] J.R. Smith, T. Perry, A. Banerjea, J. Ferrante, and G. Bozzolo, Phys. Rev. B **44**, 6444 (1991).

[26] Y.N. Devyatko and S.V. Rogozhkin, Vacuum **26**, 279 (2000).

[27] R. Ferrando, Phys. Rev. Lett. **76**, 4195 (1996).

[28] Y. Kuk and L.C. Feldman, Phys. Rev. B **30**, 5811 (1984).

[29] M. Lindroos, C.J. Barnes, and M. Valden, Surf. Sci. **218**, 269 (1989).

[30] H.L. Davis and J.R. Noonan, Surf. Sci. **126**, 245 (1983).

[31] B.W. Busch and T. Gustafsson, Surf. Sci. **407**, 7 (1998).

[32] G. Bracco, M. Canepa, P. Cantini, F. Fossa, L. Mattera, S. Terreni, and D. Truffelli, Surf. Sci. **269/270**, 61 (1992).

[33] G. Bracco, A. Pizzorno, and R. Tatarek, Surf. Sci. **377/379**, 94 (1997).

[34] L. Pedemonte, G. Bracco, R. Tatarek, M. Aschoff, K. Brning, and W. Heiland, Surf. Sci. **482-485**, 1457 (2001).

[35] F. Stietz, G. Meister, A. Goldman, and J.A. Schaefer, Surf. Sci. **339**, 1 (1995).

[36] F. Moresco, M. Rocca, V. Zielasek, T. Hildebrandt, and M. Henzler, Surf. Sci. **388**, 24 (1997).

[37] G. Bracco, L. Bruschi, L. Pedemonte, and R. Tatarek, Surf. Sci. **377/379**, 325 (1997).

[38] G. A Held, D.M. Goodstein, R.M. Feenstra, M.J. Ramstad, D.Y. Noh, and R. J Birgeneau, Phys. Rev. B **48**, 8458 (1993).

[39] C. De Giorgi, P. Aihemaiti, F. Bautier de Mongeot, C. Boragno, R. Ferrando, and U. Valbusa, Surf. Sci. **487**, 49 (2001).

[40] R. Rusponi, C. Boragno, R. Ferrando, F. Hontinfinde, and U. Valbusa, Surf. Sci. **440**, 451 (1999).

[41] G.A. Held, J.L. Jordan-Sweet, P.M. Horn, A. Mak, and R.J. Birgeneau, Phys. Rev. Lett. **59**, 2075 (1987).

[42] I.K. Robinson, E. Vlieg, H. Hornis, and E.H. Conrad, Phys. Rev. Lett. **67**, 1890 (1991).

[43] M.A. Van Hove, W.H. Weinberg, and C.-M. Chan, *Low-Energy Electron Diffraction: Experiment, Theory and Structural Determination*, Springer Series in Surface Sciences Vol. 6 (Springer-Verlag, Berlin, 1986).

[44] See Barbieri/Van Hove phase-shift package http://electron.lbl.gov/leedpack/leeadpack.html

[45] V.B. Nascimento, V.E. de Carvalho, C.M.C. de Castilho, B.V. Costa, and E.A. Soares, Surf. Sci. **487**, 15 (2001).

[46] See http://www.webelements.com

[47] J.B. Pendry, J. Phys. C **13**, 937 (1980).

[48] P. Hohenberg and W. Kohn, Phys. Rev. **136**, B864 (1964).

[49] W. Kohn and L. Sham, Phys. Rev. **140**, A1133 (1965).

[50] See the work by S. Baroni, A. Dal Corso, S. de Gironcoli, and P. Giannozzi, http://www.pwscf.org

[51] PC Linux Cluster, at the Instituto de Física/UFBA, Brazil (CTPETRO/FINEP grant).

[52] F.D. Murnaghan, Proc. Natl. Acad. Sci. U.S.A. **30**, 244 (1944).

[53] R. Landers (private communication).

[54] W. Drexel, Z. Phys. **255**, 281 (1972).

[55] J. Xie, S. de Gironcoli, S. Baroni, and M. Sheffler, Phys. Rev. B **59**, 965 (1999).

[56] W.H. Press, S.A. Teukolsky, W.T. Vetterling, and B.P. Flannery, in *Numerical Recipes in Fortran: The Art of Scientific Computing* (Cambridge Universtiy Press, Cambridge, 1992).

[57] T.S. Rahman, Z. Tian, and J.E. Black, Surf. Sci. **374**, 9 (1997).

[58] C. Bittencourt, E.A. Soares, and D.P. Woodruff, Surf. Sci. **526**, 33 (2003).

[59] C. Bittencourt, E.A. Soares, and D.P. Woodruff (private communication).

[60] A. Gerlach, G. Meisten, R. Matzdorf, and A. Goodmann, Surf. Sci. **443**, 221 (1999).

[61] S.M. Dounce, M. Yang, and H-L. Dai, Phys. Rev. B **67**, 205410 (2003).